ACS Combinatorial Science

Research Article

pubs.acs.org/acscombsci

Rapid Identification of Areas of Interest in Thin Film Materials Libraries by Combining Electrical, Optical, X-ray Diffraction, and Mechanical High-Throughput Measurements: A Case Study for the System Ni−Al

S. Thienhaus, D. Naujoks, J. Pfetzing-Micklich, D. König, and A. Ludwig*

Institute for Materials, Ruhr-Universität Bochum, 44780 Bochum, Germany

ABSTRACT: The efficient identification of compositional areas of interest in thin film materials systems fabricated by combinatorial deposition methods is essential in combinatorial materials science. We use a combination of compositional screening by EDX together with high-throughput measurements of electrical and optical properties of thin film libraries to determine efficiently the areas of interest in a materials system. Areas of interest are compositions which show distinctive properties. The crystallinity of the thus determined areas is identified by X-ray diffraction. Additionally, by using automated nanoindentation across the materials library, mechanical data of the thin films can be obtained which complements the identification of areas of interest. The feasibility of this approach is demonstrated by using a Ni−Al thin film library as a reference system. The obtained results promise that this approach can be used for the case of ternary and higher order systems.

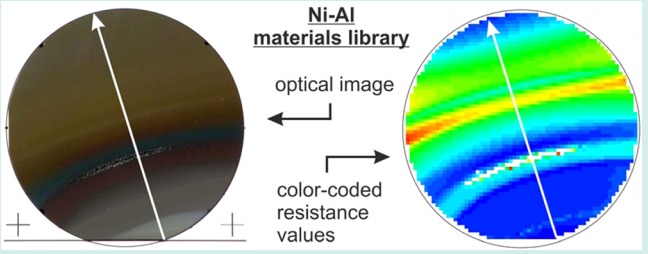

KEYWORDS: *phase identification, thin films, materials libraries, high-throughput*

INTRODUCTION

Most of the technologically interesting materials are multielement materials containing at least 3−4 alloying elements. In superalloys, more than 10 elements are used to obtain alloys with appropriate properties. In the case of thin film applications, these materials are furthermore not necessarily in their thermodynamic equilibrium. For the effective development of such compositional complex materials the combinatorial approach is essential.[1,2] While the deposition of materials libraries is well established,[3] there is a clear need for effective high-throughput methods for the rapid identification of new materials.[4]

Fabrication and processing of materials libraries allows producing a large amount of different but well-comparable samples by systematically varying parameters like chemical composition, thickness, annealing temperature, etc. To fully exploit the potential of this concept, appropriate high-throughput characterization methods have to be established that allow fast and reliable screening of the material system's properties. For exploring new material systems it is of great importance to investigate which metastable or stable crystalline phases are present in the system, how large is their compositional stability range, and to differentiate which compositional areas are single or multiphase. The standard characterization method for this structural analysis (crystallinity, phases, crystal structure) is X-ray diffraction (XRD). The drawback of this method for high-throughput characterization is that the measurement time using standard laboratory equipment is rather long (on the order of 5 to 10 min for one XRD pattern) so that measuring a materials library, which usually contains hundreds of samples, easily can take several days. Also the lateral resolution of standard XRD equipment is rather low (on the order of a few mm, in our system 2 mm × 5 mm) so that a defined measurement in one measurement area on the materials library might overlap with neighboring measurement areas. Microdiffraction provides a much higher resolution of the beam (<1 mm) but to achieve a small spot size combined with high time savings, only a synchrotron is suitable for these measurements. High-throughput analysis of materials libraries at synchrotrons has been successfully performed by many groups.[5−8] However, access to a synchrotron is limited and the screening of materials libraries for phases cannot be done on a daily basis.

In this Research Article, we propose to use a combination of compositional, electrical and optical high-throughput measurements to rapidly identify the areas of interest in a materials library. We define an area of interest as a composition region where the materials properties are considerably different (e.g., different color, different resistivity, different mechanical properties) compared to neighboring regions. This can be observed as nonlinearities of property value versus composition graphs. The crystalline phases present in the areas of interest are then determined by XRD. These measurements can be complemented by automated mechanical measurements.

Received: May 4, 2014
Revised: July 25, 2014
Published: November 3, 2014

   dx.doi.org/10.1021/co5000757 | ACS Comb. Sci. 2014, 16, 686−694

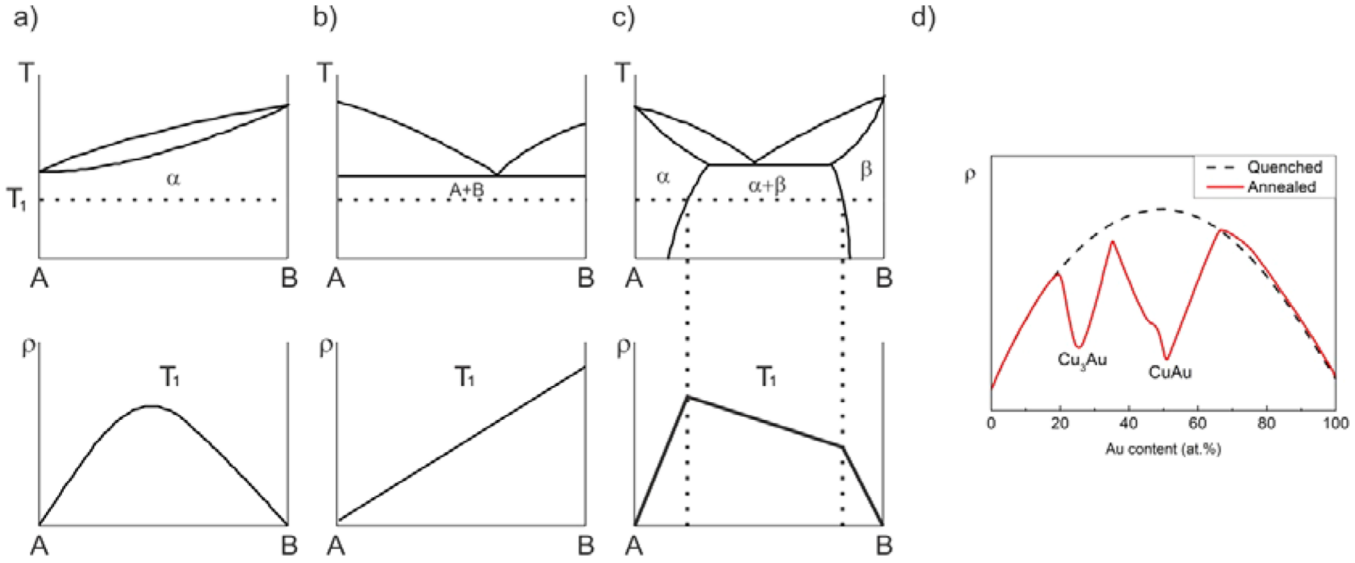

Figure 1. Schematics of resistivity-composition dependencies: (a) miscible system, (b) immiscible system, (c) limited solubility system, and (d) example of the compound forming system Cu−Au. The figures were adapted with permission from refs 9 and 11. Copyright 1985 American Society for Metals and Copyright 2007 Springer.

Principles of the Used High-Throughput Methods for the Determination of Areas of Interest. Electrical and optical measurements are appropriate for the determination of areas of interest in a materials library as these measured properties are sensitive to the structure of the material. Furthermore, they can be performed with high throughput and high spatial resolution.

In alloys, the electrical resistivity is affected by the scattering of electrons at lattice defects like voids, impurities, dislocations, grain boundaries and other interfaces (temperature independent) and by the phonon−electron interaction (temperature dependent). Figure 1 shows the generic relations between the phase diagram of binary systems and the corresponding dependence of resistivity on composition and crystal structure,[9] however neglecting any influences of microstructure on the resistivity, which might also be present. In the case of complete miscibility (Figure 1a) the resistivity increases for increasing amounts of the second element, leading to a maximum of resistivity for intermediate compositions of the solid solution. In the case of immiscible elements (Figure 1b) a linear mixture rule applies: that is, the composition-dependent resistivity is linear. Partly miscible systems with limited solubility of the second element (Figure 1c) show as well linear composition-dependent resistivity. The linear regions with different slopes connect at the solubility limits of a given temperature. These positions can be observed as kinks in the resistivity-composition diagram. In materials systems where (ordered) intermetallic compounds can form, a resistivity minimum can be observed for the compositions of the intermetallic compounds. An example is the Cu−Au system (Figure 1d). In the quenched state Cu−Au forms a solid solution, the composition-dependent resistivity is shown in Figure 1a. After the formation of the intermetallics two corresponding resistivity minima can be observed. The temperature-independent term which is affected by the defects and microstructure can be seen as a measure of the degree of order of the system: the higher the order, the lower the resistivity due to less scattering.[10] The absolute values of resistivity and the temperature dependence of the resistivity can be used to identify the material class (metal, semiconductor, insulator) of the investigated material. Finally, in the field of shape memory alloys measuring the temperature-dependent resistivity is an established method to explore the transformation behavior between the high temperature austenite phase and the low temperature martensite phase.[12] Temperature-dependent resistivity screening across thin film materials libraries was used to identify transforming regions in Ti−Ni−X systems.[13]

Another property which changes with phase constitution is the optical appearance of a material. A striking example of color change with intermetallic phase formation is the purple color of $AuAl_2$.[14] Furthermore, it was observed in a variety of thin film materials systems that after an annealing process, where phase formation was initiated, the thin film materials library changed its optical appearance in dependence of composition: colors and contrast changed differently in different compositional regions of the library, or initially reflective areas became dull. The reasons for the observed changes lie in the physical properties of the materials. In the case of metals and alloys the metallic bonding between the delocalized electrons and the positively charged metal ions affects the physical properties which include opacity and luster.[15] Roughness influences the reflectivity of a material. Oxidation might cause color changes by tarnishing or interference.

Mechanical properties also strongly depend on the phases and microstructure being present in a thin film. Solid solutions can exhibit increased strength compared to the pure metal. In two-phase regions precipitation hardening can be expected. If elements can form an intermetallic compound, whose crystal structure is different from those of the elements, the mechanical characteristics can change significantly. High-throughput nanoindentation was used as a characterization tool for mapping mechanical properties, as well as shape memory alloy compositions in combinatorial thin-film libraries.[16−20]

All the methods discussed above are able to measure properties, which are influenced by phase formation, and they are established as high-throughput measurements with a lateral resolution in the range of 1 mm or less. However, neither the electrical nor the optical or mechanical characterization method

dx.doi.org/10.1021/co5000757 | ACS Comb. Sci. 2014, 16, 686−694

is able to determine the structure of the phases present, they rather can determine their presence and the transition from one phase region to another. The identification of the phases has to be done by using XRD analysis.

In this Research Article, we discuss the combination of resistivity, optical, XRD, and mechanical screening methods for the identification of areas of interest and of (unknown) phase regions in materials systems. To validate the feasibility of this approach, a binary Ni−Al thin film materials library was fabricated as a model system and was analyzed by using the above-mentioned approach. Ni−Al was chosen as a model system because it is a well-documented system with well-known phases,[21] including the B2 phase NiAl which can show a martensitic transformation and shape memory behavior.[22] It is also the base system for Ni-based superalloys as well as bond coats for superalloys. The oxidation of Ni−Al-based bond coats was studied by combinatorial methods.[23]

EXPERIMENTAL PROCEDURES

A binary Ni−Al continuous composition spread (CCS) type thin film materials library was deposited on a thermally oxidized 4 in. (100) Si wafer (1.5 μm SiO_2 diffusion barrier) using a combinatorial magnetron sputter system (base pressure 10^{-8} mbar).[12] The CCS was fabricated using an opposing wedge-type multilayer approach.[24] Individual wedges with thicknesses of a few nm were realized by using a tilted cathode setup.[25] Repeated deposition of individual wedges led to a total nominal film thickness of 360−540 nm across the materials library. During sputtering the Ar (6N) pressure was 0.67 Pa and the Ar flow was set to 60 sccm. The deposition powers were set to 75 W (DC) and 190 W (DC) for Ni and Al, respectively. Subsequently, the multilayer thin film structure was annealed in situ at 550 °C for 1 h, in order to transform the multilayer precursor structure into an alloy. Higher temperatures were not used to avoid evaporation of Al.

The chemical compositions of the binary CCS were determined by automated energy-dispersive X-ray (EDX) measurements using a JEOL 5800LV scanning electron microscope (SEM) equipped with an Oxford INCA EDX system. A grid of 342 measurement areas was defined with spacings of 4.5 mm in x- and y-direction. The total EDX measurement time for a materials library is about 8−10 h.

Automated high-throughput resistance measurements were performed using a custom-built high-throughput measurement test stand. The test stand is equipped with a 4-point probe head with spring-loaded contact pins having a pin-to-pin distance of 0.5 mm to achieve a sufficient lateral resolution. Further details to this measurement technique can be found in.[4] The measurement current (DC) was set to 50 mA, step width was 1.5 mm in x- and y-direction. With these parameters the measurement of 3389 points on the 4 in. diameter materials library takes about 5 h.

For the optical characterization of the materials library an image with an 8 megapixel digital camera was taken. From the image the RGB values were extracted from the jpeg data. Because of the high reflectivity of thin film libraries deposited on Si wafers, it is challenging to take a picture. Depending on the lighting conditions, the angle between camera and materials library, background color, camera settings, etc., pictures of the same materials library can appear differently when these conditions change. Therefore, a photostand was set up which allows to take a picture of a materials library always under the same conditions with optimized surroundings in a reproducible way. The photostand consists of a black box where the positions of the camera and the materials library are fixed (Figure 2). The camera is placed at a distance of about 1.5 m

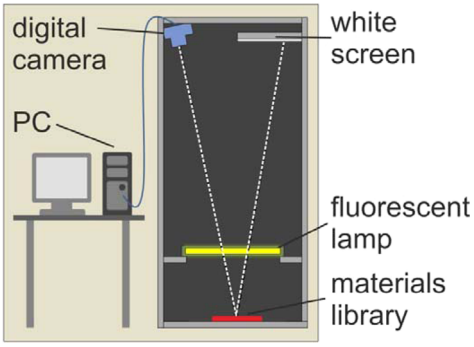

Figure 2. Schematic of the photostand setup. While taking a picture the photostand is covered with black cloth to exclude external optical influences.

from the materials library, tilted under an angle of about 5°, to avoid a mirror image of the camera on the picture and to avoid distortions of the circular materials library which occurs when the tilt-angle becomes too large. Two fluorescent lamps (8 W, 4200 K) are installed opposite to each other close to the materials library. To avoid reflections from the materials library, a homogeneous white screen was installed as a background. When the picture is taken the box is closed to exclude external optical influences. To be able to correlate the RGB values with data from other measurements like chemical composition (EDX), structure (XRD), resistance etc., reference marks are placed next to the materials library, which are later used to define a grid across the library. A Matlab based software was programmed which allows extracting the RGB values from the picture at the coordinates which correspond to the measurement grid of other high-throughput measurements. The analysis of pictures taken at the photostand is versatile and can be used for other measurements: for example, in conjunction with a hot plate, phase transformations, or oxidation behavior of materials libraries can be characterized.

Young's modulus and hardness of the materials library were measured using high-throughput nanoindentation:[19] a nanoindenter (XP, MTS) with a Berkovich tip and a standard method involving continuous stiffness measurement (CSM) with a frequency of 45 Hz and amplitude of 2 nm was used. Maximum displacement of the performed indentations was 100 nm, Young's modulus and hardness values were analyzed between 50 and 80 nm indentation depth with a strain rate of 0.05 1/s. As the indentation depths were much smaller than the film thickness, substrate effects could be neglected. For each investigated composition five indentations were performed and average values and standard deviations were calculated. The measurement of 30 compositions on the materials library took about 20 h.

Automated XRD measurements along the compositional gradient of the Ni−Al materials library were used to reveal the crystal structure and the phases present in the system. The measurements were performed using a PANalytical XPert MRD system (Cu K_α radiation, acceleration voltage 45 kV, heating current 40 mA). In the case study of the binary materials library the measurement time for the line scan took

dx.doi.org/10.1021/co5000757 | ACS Comb. Sci. 2014, 16, 686−694

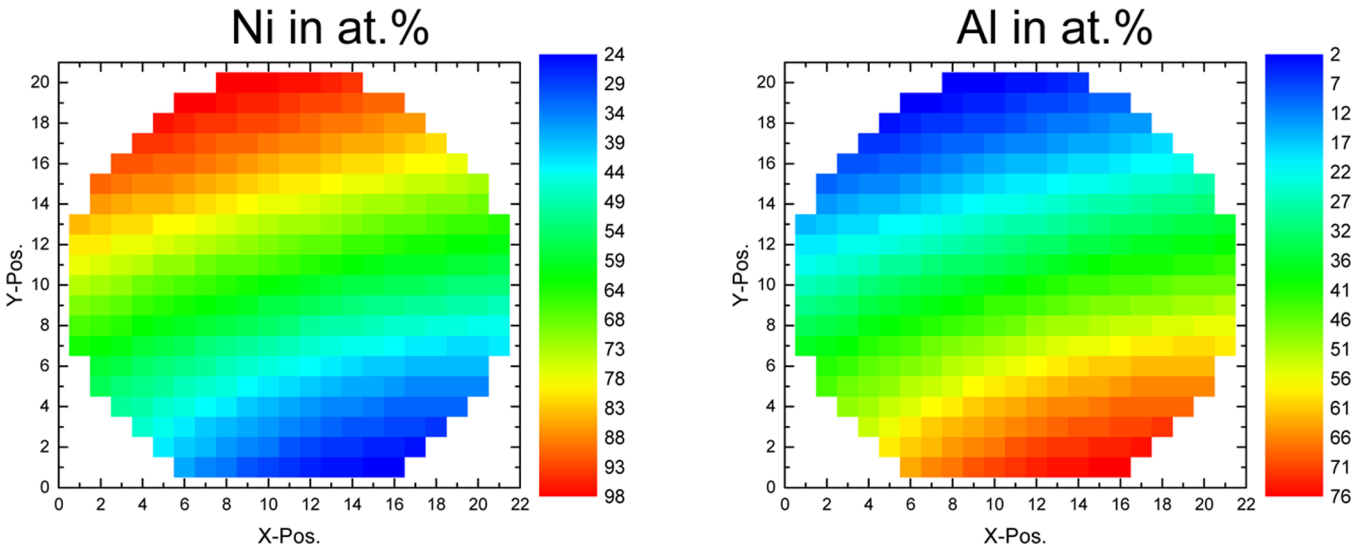

Figure 3. Color-coded composition distribution of Ni and Al, respectively, across the 4 in. materials library. 342 positions (d*x*, d*y* = 4.5 mm) were measured by automated EDX.

about 5 h (measurement time per measurement area was about 10 min).

RESULTS

In the following the results of compositional, resistivity, optical and mechanical screenings are presented together with the structural analysis performed by XRD.

The results of the automated EDX measurement of the Ni–Al materials library based on 342 measurement points show the distribution of the elements across the 4 in. wafer (Figure 3). While the Ni-amount ranges from 24 to 98 at. %, the Al-amount ranges from 2 to 76 at. %, respectively. The error of this measurement lies in the range of ±0.5 at. %. The compositional gradient is in the range of about 0.8 at. % per mm and is slightly tilted toward the axis which lies perpendicular to the wafer flat. This is due to the orientation between the substrate and the sputter cathodes. Figure 3 shows also that the elemental distribution in the direction perpendicular to the composition gradient is slightly curved. This is a result of the natural film thickness distribution resulting from the sputter deposition from 4 in. targets on 4 in. substrates.

Figure 4 shows the results of the resistance mapping of the materials library. It can be observed qualitatively that there are distinct regions of high and low resistance. The reason that the regions of similar resistance are curved across the materials library is again related to the sputter process and the fact that toward the edges of the substrate the sputter profile is not homogeneous (see above). For the binary system under investigation further analysis was performed only in the area indicated by the white arrow as shown in Figure 4. This is due to delamination, probably due to high stress in the film, which occurred toward the center of the materials library where no measurements were possible (missing points in Figure 4).

Figure 5 shows the resistance values along the white arrow of Figure 4. Four local maxima (at measured compositions of $Ni_{27}Al_{73}$, $Ni_{47}Al_{53}$, $Ni_{70}Al_{30}$, $Ni_{81}Al_{19}$) and three local minima (at measured compositions of $Ni_{40}Al_{60}$, $Ni_{52}Al_{48}$, $Ni_{76}Al_{24}$) were observed along the measured resistance values (marked by straight lines, filled triangles). Furthermore, at least three inflection points (marked by dotted lines, open triangles) can

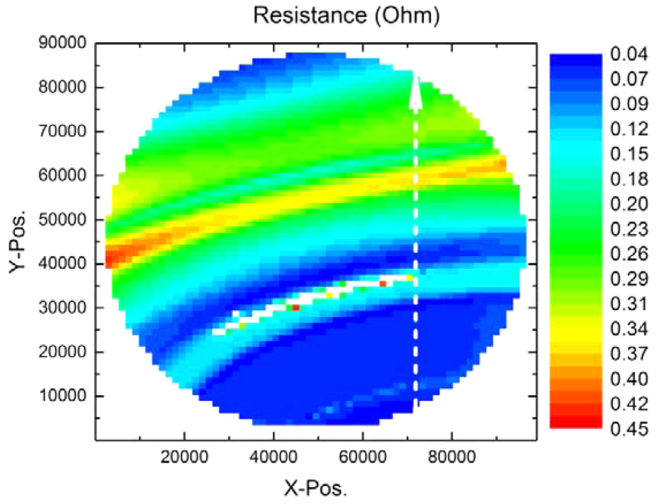

Figure 4. Results of the resistance measurement across the Ni–Al materials library, based on 3389 measurement points (d*x*, d*y* = 1.5 mm). Further characterization was performed in the area indicated by the white arrow.

be observed at the compositions of about $Ni_{44}Al_{56}$, $Ni_{57}Al_{43}$, and $Ni_{66}Al_{34}$. According to the principles of the resistivity-composition dependencies as shown in Figure 1, these distinctive features are used in the following analysis to define probable phase regions within the composition spread. These regions are then compared to the regions which were assessed by analysis of the optical, mechanical and XRD measurements.

Figure 6a shows the picture of the annealed Ni–Al thin film materials library. For better distinction, the picture colors were modified by adjusting color saturation, contrast, and gamma values. The picture of the materials library shows different colored stripe regions (white, gray, red, blue, and yellow), which lie approximately perpendicular to the concentration gradient across the materials library. Between the red and blue stripe there is a small region where delamination of the film occurred. Due to this damaged region further analysis was carried out along the white dotted arrow. Figure 6b shows the RGB-values along the arrow, starting at the Al-rich end of the

dx.doi.org/10.1021/co5000757 | ACS Comb. Sci. 2014, 16, 686–694

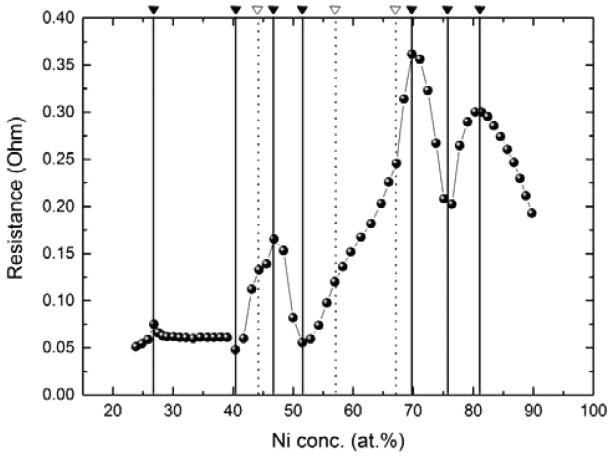

Figure 5. Measured resistance values in dependence of composition (along the white arrow of Figure 4), showing 7 minima and maxima (filled triangles), as well as 3 inflection points (open triangles).

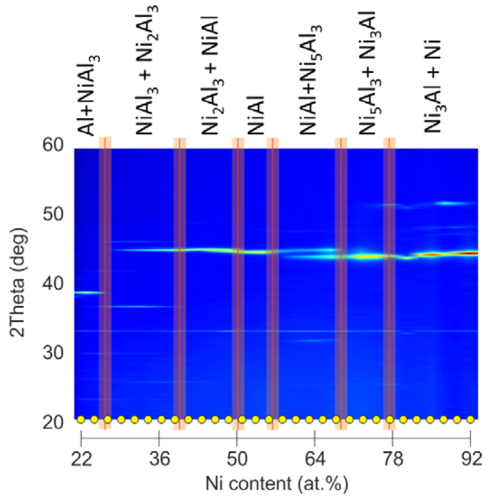

Figure 7. Visualization of 30 XRD patterns taken along the compositional gradient (white arrow in Figure 6a) from $Ni_{22}Al_{78}$ to $Ni_{92}Al_8$ (blue, low; red, high peak intensity). The broad red lines indicate the phase boundaries of the identified phase regions, which are given on top of the figure.

materials library. Figure 6a suggests that some of the colored stripes show a continuous transition into the next color region. However, when looking at the RGB values in Figure 6b the color regions can be distinguished and boundaries can be identified. The positions of the boundaries were determined qualitatively by judging the color changes by eye. These boundaries do not necessarily fall on minima or maxima values of the composition-dependent RGB values. The vertical lines in Figure 6b indicate the boundaries between these regions of different color. Similar to the resistance data which was divided into regions by identifying the resistance minima and maxima, the optical data was divided into regions by identifying differently colored regions. Nine regions with different colors were identified along the white arrow.

A detailed phase analysis by automated XRD measurements at 30 measurement positions on the materials library was performed along the white arrow of Figure 6 a), using a step size of 3 mm. The results of these measurements were visualized using the XRD-Suite software[26] and are summarized in Figure 7. According to the bulk phase diagram (APDIC), the Ni−Al system has seven stable phases: Al, $NiAl_3$, Ni_2Al_3, NiAl, Ni_5Al_3, Ni_3Al, and Ni.[27] Peaks corresponding to these phases were identified in the measured XRD patterns. However, because the spot size of the XRD measurement is in the same range as the step size (~3 mm) between XRD measurement areas, there is a small overlap between the measurements. Therefore, the boundaries of the phase regions in Figure 7 are depicted as broad lines. This also means, that due to the low lateral resolution, single phase regions that extend over a range of only a few at.% cannot be resolved. According to the Ni−Al bulk phase diagram at 550 °C the single phases $NiAl_3$, Ni_2Al_3, Ni_5Al_3, and Ni_3Al exist only in narrow compositional regions ($NiAl_3$ is a line-phase, width of the Ni_2Al_3 phase, ~4 at. %; width of the Ni_5Al_3 phase, ~3 at. %; width of the Ni_3Al phase, <2 at. %). This explains why only one single-phase region,

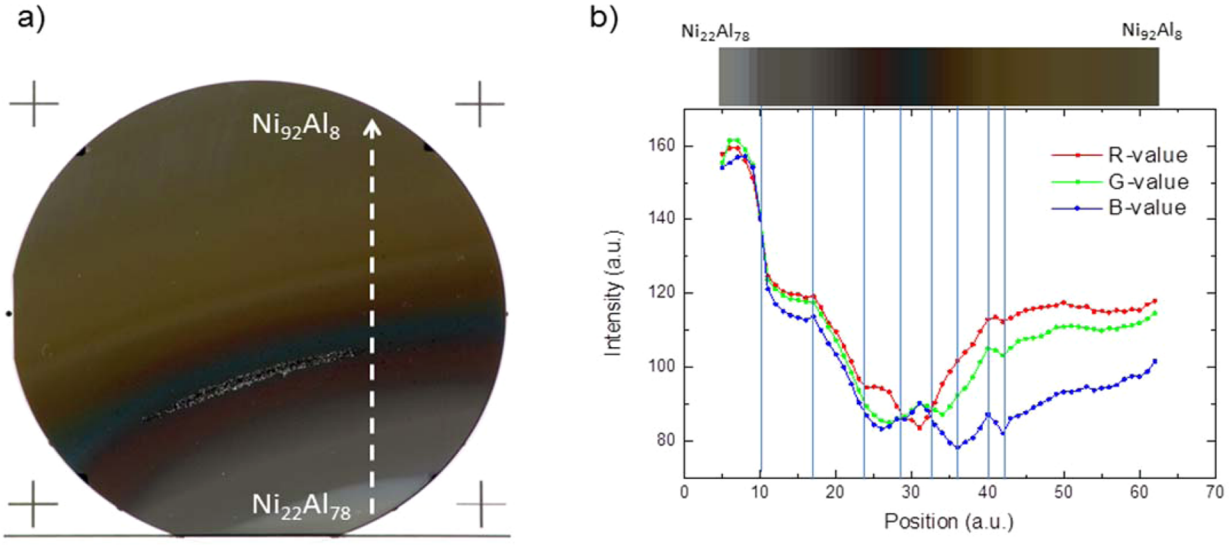

Figure 6. (a) Picture of a Ni−Al thin film materials library deposited on a 4-in. oxidized Si-wafer (colors optimized). The crosses are reference marks enabling spatial correlation of the optical data with other measurements. (b) Composition-dependent RGB-values along the arrow of panel a) starting at the Al-rich end of the materials library.

dx.doi.org/10.1021/co5000757 | ACS Comb. Sci. 2014, 16, 686−694

namely NiAl, was observed. The NiAl phase in the thin film materials library only extends over the Ni range of 51.6−54.2 at. %, which is narrower than the phase expansion in the bulk system which extends over a much larger region (~14 at. %). The reason for this might be that the phase equilibrium in the thin film has not been reached and therefore the bulk phase diagram is not fully comparable to the thin film case.

In Figure 8, the results from nanoindentation measurements are shown. The tendencies of the measured Young's modulus and hardness with composition are identical. At low Ni contents, Young's modulus and hardness values are around 140 and 5.5 GPa, respectively. Both values increase with increasing Ni concentration reaching maximum values of 230 and 16 GPa, respectively. When maximum values are reached, a narrow region appears (Ni-concentration between 43 and 51 at. %) where the thin film library peeled off, so that nanoindentation measurements could not give reliable data. At $Ni_{55}Al_{45}$ the mechanical values show a local maximum, followed by a local minimum at about $Ni_{60}Al_{40}$ (Young's modulus 166 GPa, hardness 7 GPa). With increasing Ni content Young's modulus and hardness increase reaching another local maximum at $Ni_{71}Al_{29}$ (Young's modulus 205 GPa, hardness 14 GPa). At $Ni_{76}Al_{24}$, there is a local minimum after a steep decrease of the values. After a local maximum at $Ni_{79}Al_{21}$, the values for Young's modulus and hardness decrease with increasing Ni content.

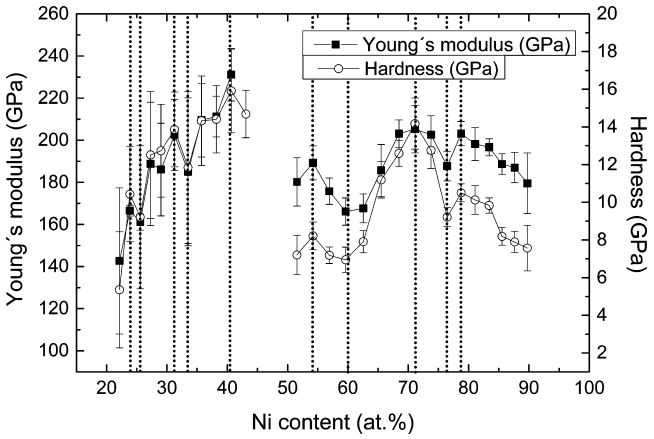

Figure 8. Results of the nanoindentation measurements for Young's modulus and hardness. (For Ni concentrations from 43 to 52 at. % the thin film library could not be measured because of peeling of the film). Local maxima and minima are marked with dotted lines.

DISCUSSION

The results shown above illustrate that the high-resolution screening methods (resistivity, optical, mechanical) yield data with clear nonlinearities (maxima, minima, inflection points) on which the determination of areas of interest in materials libraries can be based. The correlation of the different screening results is analyzed in the following.

Figure 9 shows the direct comparison between the optical image and the color-coded resistance values across the materials library, as well as the compositional data. The differently colored regions of the optical image correspond well with the regions of similar resistance values and similar composition.

The XRD structure data, together with the resistance data and the results from the mechanical measurements, was then correlated with the color data extracted from the picture of the materials library using Matlab-based software. Results of this comparison are shown in Figure 10. For better comparability, all data has been normalized and an offset has been added. Since there is a concentration gradient across the materials library (74 at. % over 93 mm) and the lateral resolution of the XRD measurement is in the range of 3 mm, the correlation of the phase boundaries and the Ni-content implies an error of about ±1.2 at. %, which is the reason that the phase boundaries are not plotted as sharp lines.

In the following, the data is discussed for increasing Ni content. The two phase region (Al + $NiAl_3$) which extends up to a Ni content of approximately 28 at. % corresponds well with the white colored area of the materials library (highest RGB-values). At the boundary to the two phase region ($NiAl_3$ + Ni_2Al_3) there is steep descent of the RGB-values (transition from white to gray) which coincides with a local maximum of the resistance value and a local minimum in the Young's modulus as well as in the hardness values. At a Ni-content of about 33−34 at. % the RGB-values show an inflection point, and the values of the Young's modulus and hardness show a local minimum while the resistance values are constant in this concentration range. The XRD analysis did not show any change of phases at this Ni concentration. At the phase boundary between ($NiAl_3$+Ni_2Al_3) and (Ni_2Al_3+NiAl) the RGB-values separate, which corresponds to the transition from the gray to a red region on the materials library. This happens at a Ni-concentration of about 41 at. % where the resistance

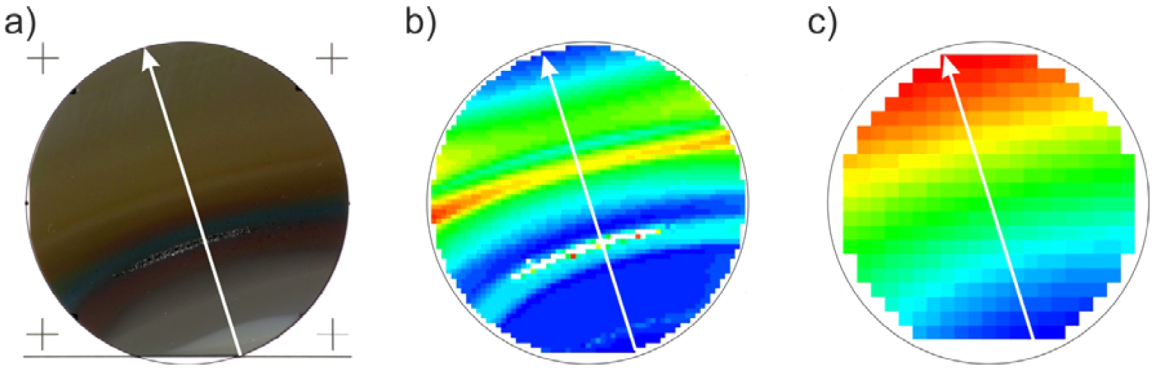

Figure 9. Comparison of the (a) optical image, (b) the color-coded resistance values (3389 measurement areas), and the (c) Ni-content (color-coded) across the complete Ni−Al materials library (342 measurement areas). The white arrow indicates the concentration gradient across the complete materials library ($Ni_{24}Al_{76}$ to $Ni_{98}Al_2$).

dx.doi.org/10.1021/co5000757 | ACS Comb. Sci. 2014, 16, 686−694

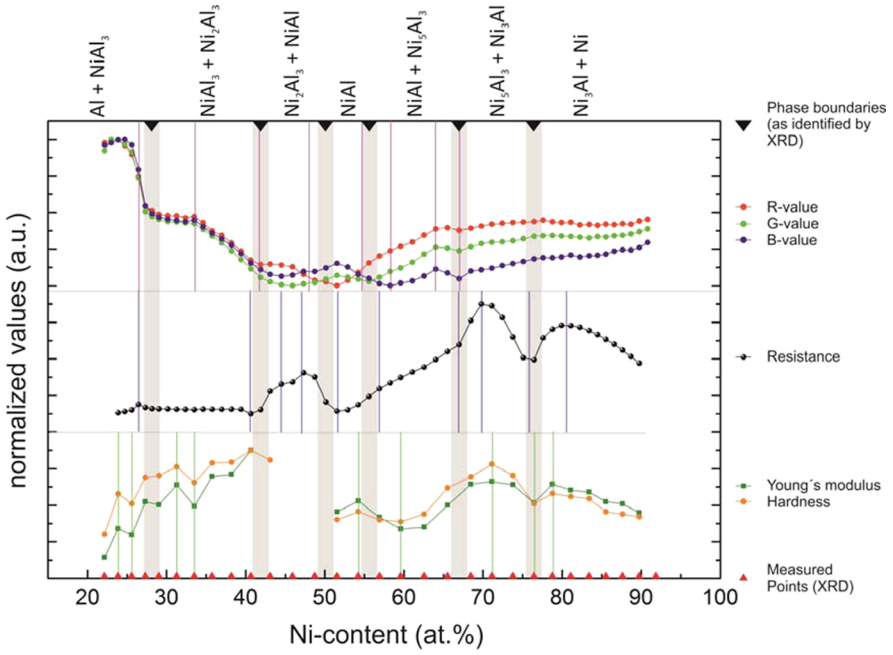

Figure 10. Results of the optical, electrical, and mechanical measurements, correlated with the results of the structure analysis by XRD (all values normalized for better comparability). The vertical gray bars correspond to the phase region boundaries as identified by XRD. The red marks show the positions at which XRD and nanoindentation measurements were performed. The pink, blue, and green vertical lines correspond to the compositions of interest of the optical, electrical, and mechanical measurements, respectively.

values show a local minimum and Young's modulus and hardness values show a maximum. Between a Ni-content of about 43 at. % and about 51 at. % no values for Young's modulus and hardness could be measured due to delamination of the film. At the composition $Ni_{47}Al_{53}$ the color of the materials library changes from red to blue. This color change coincides with a local maximum in the resistance values. At a Ni-content around 50 at. % XRD analysis showed a phase boundary between the phase regions (Ni_2Al_3 + NiAl) and NiAl. A local minimum of the resistance values at approximately 51 at. % falls into the single phase NiAl region. At a Ni-concentration of 54−55 at. % the transition from the blue region into a red region starts corresponding to an inclining *R*-value and declining G- and B-values. At the same Ni-concentration the Young's modulus and hardness values show a local maximum. This is the concentration where the NiAl single phase region changes to the two phase region of (NiAl + Ni_5Al_3). The red region turns into orange for Ni > 60 at. %, which coincides with a local minimum in Young's modulus and hardness. A local maximum in the RGB-values appearing at about $Ni_{65}Al_{35}$ corresponds to a point of inflection in the values of Young's modulus and hardness. At a slightly higher concentration at $Ni_{68}Al_{32}$ the RGB-values have a local minimum, which coincides with an inflection point in the resistance data and the phase boundary between (NiAl + Ni_5Al_3) and (Ni_5Al_3 + Ni_3Al). In the two phase region (Ni_5Al_3 + Ni_3Al), the resistance value and the mechanical properties each show a local maximum, while the RGB-values showed no color change. At about $Ni_{75}Al_{25}$ there is a sharp drop-off of the resistance value and a distinctive local minimum in the Young's modulus and hardness. This is also the phase boundary between the (Ni_5Al_3 + Ni_3Al) and (Ni_3Al + Ni) regions. The RGB-values show no change at this Ni-concentration. At about 80 at. % Ni there is another local maximum in the resistance values and mechanical property values which lie in the two phase region of (Ni_3Al + Ni).

We have proposed that using a combination of optical and resistivity data should give a rapid indication of the areas of interest in a materials library. The present work focuses on the binary system Ni−Al to introduce the concept of this approach for finding areas of interest. For a binary system, a linescan across the materials library with distances between the measurement areas in our case of 1.5 to 4.5 mm yielded useful results (Figure 10). In a ternary or higher order system, a linescan will not be sufficient and area scans have to be performed. Table 1 gives an overview of the necessary measurement times when comparing a linescan of a binary and an area scan of a ternary (or higher order) materials library over a 100 mm diameter library substrate. Taken a distance between the measurement areas of 3 mm, this results in 30 versus 700 measurement areas, respectively. In the case of a ternary system, for example, XRD mapping (for identifying phases) would require about 5 days (for a lab system), whereas

Table 1. Overview of Measurement Times for Binary and Higher Order Systems Assuming a Distance of 3 mm between Measurement Areas Across a 100 mm Diameter Library Substrate (5 mm Border for Handling)

	binary system (line scan, 30 measurement areas)	ternary or higher order system (area scan, 700 measurement areas)
optical characterization	1 s	1 s
resistivity screening	2.5 min	1 h
automated EDX	30 min	20 h
automated XRD	5 h	116 h (5 d)
automated nanoindentation	20 h	465 h (19 d)

dx.doi.org/10.1021/co5000757 | *ACS Comb. Sci.* 2014, 16, 686−694

the combined compositional/optical/resistivity measurements take less than 24 h. The advantage of the approach is that the most interesting areas on a materials library can be identified within hours, not days. Furthermore, the optical and resistivity data is of interest, irrespective of the other measurements.

It is already obvious in the binary case that nanoindentation requires too long measurement times for the rapid identification of areas of interest in a materials library. However, it is indispensable for the high-throughput acquisition of mechanical data of thin film materials libraries.

CONCLUSIONS AND OUTLOOK

A Ni−Al thin film materials library was fabricated and subsequently annealed for phase formation. Automated resistance and nanoindentation measurements and an optical measurement were performed to validate these techniques for the identification of existing phase regions. The resulting identification of areas of interest was verified by automated XRD measurements.

For the optical measurement, a photostand was set up which allows to take pictures of thin film materials libraries under repeatedly identical conditions. In the course of the RGB value analysis, nine regions (eight boundaries) were defined which correspond to a certain color. By comparing these regions with the seven phase regions (six phase boundaries) as identified by XRD measurements, we found that five out of six phase boundaries were in accordance with each other. However, two distinctive features were found within the RGB values that do not correspond to any phase region. At a Ni-concentration of around 33 at. % the RGB-values show a distinctive inflection point which coincides with a local minimum in the mechanical properties, but the XRD analysis showed no changes for this concentration range. At a Ni concentration of about 75 at. %, which was identified by XRD to be the phase boundary of (Ni_5Al_3+Ni_3Al) and (Ni_3Al+Ni) no distinctive RGB features (no color changes) could be observed.

For the composition-dependent resistance values local minima/maxima and inflection points were used to define regions which were correlated with the phase regions identified by XRD measurements. All three identified minima could be correlated with the identified phases. When comparing the maxima and inflections points with the phase boundaries as identified by XRD three out of seven features could be correlated.

In the case of the mechanical measurements, the correlation between the detected local minima/maxima and inflection points of the Young's modulus and hardness values with possible phases is difficult: The error of the measurements (see Figure 7) is in the range of the identified local minima and maxima. Despite this, correlations exist like the decrease in Young's modulus and hardness at around $Ni_{76}Al_{24}$, which is right at a phase boundary identified with XRD. The fact that the Young's modulus values, as well as the hardness values increase with increasing Ni-content and reach a maximum at around $Ni_{40}Al_{60}$ might coincide with a buildup of inner stress, which finally led to the delamination of the film in the Ni-range between 43 and 51 at. %, where no measurements could be performed.

The combination of optical and resistivity screening is useful for the rapid identification of areas of interest in thin film materials libraries, as well as to get information on functional properties, as these two methods provide both high speed and high spatial resolution. In combination with XRD, the crystallinity of these areas can be determined efficiently. It is intended to use this method for the exploration of the compositional spaces of phases in ternary subsystems (Ni−Al−Cr, Co−Al−W) of superalloys or other compositionally complex materials systems.

AUTHOR INFORMATION

Corresponding Author

*E-mail: alfred.ludwig@rub.de.

Notes

The authors declare no competing financial interest.

ACKNOWLEDGMENTS

This work was supported by the German Research Foundation (DFG) through project B5 in the framework of SFB/Transregio 103. The support from C. Sure is acknowledged for his contribution for the setup of the photostand.

REFERENCES

(1) Takeuchi, I.; Lauterbach, J.; Fasolka, M. J. Combinatorial materials synthesis. *Mater. Today* **2005**, *8* (10), 18−26.

(2) Zhao, J. C. A Combinatorial Approach for Structural Materials. *Adv. Eng. Mater.* **2001**, *3* (3), 143−147.

(3) Ludwig, A.; Zarnetta, R.; Hamann, S.; Savan, A.; Thienhaus, S. Development of multifunctional thin films using high-throughput experimentation methods. *Int. J. Mater. Res.* **2008**, *99* (10), 1144−1149.

(4) Thienhaus, S.; Hamann, S.; Ludwig, A. Modular high-throughput test-stand for versatile screening of thin-film materials libraries. *Sci. Technol. Adv. Mater.* **2011**, *12*, No. 054206.

(5) Green, M. L.; Takeuchi, I.; Hattrick-Simpers, J. R. Applications of high throughput (combinatorial) methodologies to electronic, magnetic, optical, and energy-related materials. *J. Appl. Phys.* **2013**, *113*, No. 231101.

(6) Chu, Y. S.; Tkachuk, A.; Vogt, S.; Ilinski, P.; Walko, D. A.; Mancini, D. C.; Dufresne, E. M.; He, L.; Tsui, F. Structural investigation of CoMnGe combinatorial epitaxial thin films using microfocused synchrotron X-ray. *Appl. Surf. Sci.* **2004**, *223*, 175−182.

(7) Gao, T. R.; Wu, Y. Q.; Fackler, S.; Kierzewski, I.; Zhang, Y.; Mehta, A.; Kramer, M. J.; Takeuchi, I. Combinatorial exploration of rare-earth-free permanent magnets: Magnetic and microstructural properties of Fe−Co−W thin films. *Appl. Phys. Lett.* **2013**, *102*, No. 022419.

(8) Zarnetta, R.; Takahashi, R.; Young, M. L.; Savan, A.; Furuya, Y.; Thienhaus, S.; Maaß, B.; Rahim, M.; Frenzel, J.; Brunken, H.; Chu, Y. S.; Srivastava, V.; James, R. D.; Takeuchi, I.; Eggeler, G.; Ludwig, A. Idenfication of Quaternary Shape Memory Alloys with Near-Zero Thermal Hysteresis and Unprecedented Functional Stability. *Adv. Funct. Mater.* **2010**, *20*, 1917−1923.

(9) Pollock, D. D. *Electrical Conduction In Solids: An Introduction*; American Society for Metals: Materials Park, OH, 1985.

(10) Rossiter, P. L. *The Electrical Resistivity of Metals and Alloys*; Cambridge University Press: Cambridge, U.K., 1991.

(11) Koughia, C.; Kasap, S.; Capper, P. *Springer Handbook of Electronic and Photonic Materials*; Springer: New York, 2007, 27.

(12) Löbel, R.; Thienhaus, S.; Savan, A.; Ludwig, A. Combinatorial fabrication and high-throughput characterization of a Ti−Ni−Cu shape memory thin film composition spread. *Mater. Sci. Eng. A* **2008**, *481−482*, 151−155.

(13) Zarnetta, R.; Buenconsejo, P. J. S.; Savan, A.; Thienhaus, S.; Ludwig, A. High-throughput study of martensitic transformations in the complete Ti−Ni−Cu system. *Intermetallics* **2012**, *26*, 98−109.

(14) Cahn, R. W. A precious stone that isn't. *Nature* **1998**, *396*, 523−524.

(15) Tilley, R. J. D. *Colour and the Optical Properties of Materials: An Exploration of the Relationship between Light, the Optical Properties of Materials and Colour*, 2nd ed.; Wiley: Chichester, U.K., 2011; p 419.

(16) Warren, O. L.; Wyrobek, T. J. Nanomechanical property screening of combinatorial thin-film libraries by nanoindentation. *Meas. Sci. Technol.* **2005**, *16*, 100−110.
(17) Yoo, Y. K.; Xue, Q.; Chu, Y. S.; Xu, S.; Hangen, U.; Lee, H.-C.; Stein, W.; Xiang, X.-D. Identification of amorphous phases in the Fe−Ni−Co ternary alloy system using continuous phase diagram material chips. *Intermetallics* **2006**, *14* (3), 241−247.
(18) Dwivedi, A.; Wyrobek, T. J.; Warren, O. L.; Hattrick-Simpers, J.; Famodu, O. O.; Takeuchi, I. High-throughput screening of shape memory alloy thin-film spreads using nanoindentation. *J. Appl. Phys.* **2008**, *104*, No. 073501.
(19) Zarnetta, R.; Kneip, S.; Somsen, C.; Ludwig, A. High-throughput characterization of mechanical properties of Ti−Ni−Cu shape memory thin films at elevated temperatures. *Mater. Sci. Eng. A* **2011**, *528*, 6552−6557.
(20) Han, S. M.; Shah, R.; Banerjee, R.; Viswanathan, G. B.; Clemens, B. M.; Nix, W. D. Combinatorial studies of mechanical properties of Ti−Al thin films using nanoindentation. *Acta Mater.* **2005**, *53*, 2059−2067.
(21) Ishida, K.; Kainuma, R.; Ueno, N.; Nishizawa, T. Ductility Enhancement in NiAI (B2)-Base Alloys by Microstructural Control. *Metall. Trans. A* **1991**, *22*, 441−446.
(22) Myagkov, V. G.; Bykova, L. E.; Zharkov, S. M.; Bondarenko, G. N. Formation of NiAl Shape Memory Alloy Thin Films by a Solid-State Reaction. *Solid State Phenom.* **2008**, *138*, 377−384.
(23) Metting, C. J.; Bunn, J. K.; Underwood, E.; Smoak, S.; Hattrick-Simpers, J. Combinatorial Approach to Turbine Bond Coat Discovery. *ACS Comb. Sci.* **2013**, *15*, 419−424.
(24) Buenconsejo, P. J. S.; Zarnetta, R.; Ludwig, A. The effects of grain size on the phase transformation properties of annealed (Ti/Ni/W) shape memory alloy multilayers. *Scr. Mater.* **2011**, *64* (11), 1047−1050.
(25) Hamann, S.; Gruner, M. E.; Irsen, S.; Buschbeck, J.; Bechtold, C.; Kock, I.; Mayr, S. G.; Savan, A.; Thienhaus, S.; Quandt, E.; Fähler, S.; Entel, P.; Ludwig, A. The ferromagnetic shape memory system Fe−Pd−Cu. *Acta Mater.* **2010**, *58* (18), 5949−5961.
(26) Long, C. J.; Hattrick-Simpers, J.; Murakami, M.; Srivastava, R. C.; Takeuchi, I.; Karen, V. L.; Li, X. Rapid structural mapping of ternary metallic alloy systems using the combinatorial approach and cluster analysis. *Rev. Sci. Instrum.* **2007**, *78*, No. 072217.
(27) Massalski, T. B. *Binary Alloy Phase Diagrams*, 2nd ed.; ASM International: Materials Park, OH, 1990; Vol. *1*, ppp 181−184.